



Phase control of all-optical switching based on spontaneously generated coherence in a three-level Λ -type atomic system

Nguyen Thi Thu Hien^{1,2}, Nguyen Tuan Anh¹, Nguyen Huy Bang², Dinh Xuan Khoa², Le Van Doai², Ho Hai Quang², and Hoang Minh Dong^{1,a} 

¹ Ho Chi Minh City University of Food Industry, Ho Chi Minh City, Vietnam

² Vinh University, 182 Le Duan Street, Vinh City, Vietnam

Received 20 May 2022 / Accepted 25 October 2022

© The Author(s), under exclusive licence to EDP Sciences, SIF and Springer-Verlag GmbH Germany, part of Springer Nature 2022

Abstract. Controllable all-optical switching by relative phase and spontaneously generated coherence in a three-level Λ -type atomic system is our aim in this study. We have generated a near-square probe pulse train with a similar modulation period through periodic modulation of the relative phase or coupling field intensity. Results show that the spontaneously generated coherence and phase range have a strong influence on the efficiency and shape of the switching pulse. Furthermore, the phase switching performance is enhanced as spontaneously generated coherence increases with incoherent pumping. In addition, synchronous or asynchronous switching of the probe pulse is observed in different phase domains ($0-\pi$ or $\pi-2\pi$). The studied scheme may be helpful for use in the design of optical switching devices in optical communications.

1 Introduction

All-optical switching (AOS) is a very important element in optical communication systems, optical data processing and quantum computers [1]. However, the basic research on optical switching has not yet met the requirements for practical devices that require low switching power, high switching speed and low signal loss. In the past several decades, the discovery of electromagnetically induced transparency (EIT) [2, 3] has yielded atomic materials with giant nonlinearities and very small absorption in the resonance domain [4, 5]. As a result, EIT materials have created a number of breakthrough applications in quantum and nonlinear optics, such as slow light [6], optical storage devices [7], optical bistability [8], lasing without inversion [9], Kerr nonlinearity [10, 11] and quantum logic gates [12]. In particular, EIT materials can also alter the dynamic processes of light pulse propagation and create optical solitons [13–21], which is the key basis for creating AOS with low threshold intensity and super-high switching speed. For example, a number of typical studies on AOS based on EIT have been published recently [22–29]. These precursor studies have shown that the switching speed and efficiency of the probe light can be changed by adjusting the intensity or frequency of the coupling laser.

Besides the dependence of the EIT on the intensity and frequency of the coupling laser, the phase

and polarization of the light fields have a significant influence on the EIT. In particular, the combination of polarization with non-orthogonality of electric dipole moments can produce spontaneously generated coherence (SGC) [30]. Under EIT conditions, the atomic optical properties also become extremely sensitive to the changes in the SGC and the relative phase of the laser fields. Therefore, the study also investigated the influence of the SGC and the relative phase on the lasing without population inversion (LWI) [31], dispersion and absorption properties [32–36], light group velocity [37, 38], Kerr nonlinearity [39, 40], optical bistability and optical switching at low light levels [41, 42] in the steady-state domain.

Up to now, studies on the optical properties of a medium under the influence of SGC and the relative phase have been conducted mainly in the steady-state regime [30–42]. However, such studies are still limited to the dynamics of the pulse propagation process that plays an essential role in optical communication and optical switching [22–29, 43, 44]. To provide a more in-depth understanding in this direction, we propose the use of a three-level Λ -type atomic model to investigate AOS under the influence of the SGC and the relative phase. The results are obtained by numerically solving the coupled Maxwell-Bloch equations on the spatiotemporal grid and show that the output status of the probe field can be switched on or off by modulating the relative phase and the coupling field.

^a e-mail: dong.gvtvmt@gmail.com (corresponding author)

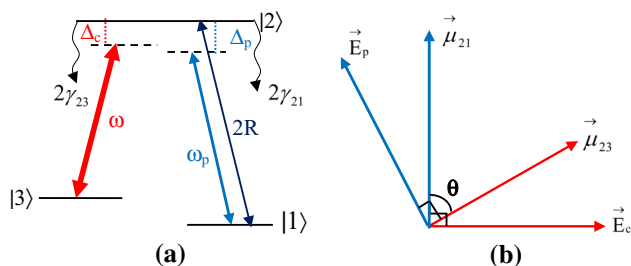


Fig. 1 **a** The three-level atomic model under the interaction of two laser fields has nearly equidistant lower levels. **b** The scheme of the polarization vector and the corresponding laser field is established such that each laser affects only one transition

2 Model and basic equations

The system under consideration consists of two laser fields interacting with a three-level Λ -type atomic medium as depicted in Fig. 1a. A weak probe laser field with carrier frequency ω_p and Rabi frequency $\Omega_1 = \mu_{21}E_p/\hbar$ is applied to the transition $|1\rangle$ to $|2\rangle$, while the transition $|2\rangle$ to $|3\rangle$ is facilitated by a strong coupling laser field with carrier frequency ω_c and Rabi frequency $\Omega_2 = \mu_{23}E_c/\hbar$. Here, μ_{ij} denotes the dipole moment for the transition $|i\rangle \rightarrow |j\rangle$, and E_p and E_c are the amplitude of the probe and coupling laser fields, respectively. Incoherent pumping is put into the system with a pump rate of $2R$ between levels $|1\rangle$ and $|2\rangle$. The orientation of the electric dipole moments $\vec{\mu}_{21}$ and $\vec{\mu}_{23}$ are shown in Fig. 1b when these dipole moments are not orthogonal to each other, which is necessary for the existence of the SGC effect. Here, each field affects only one transition; therefore, we can choose the strong coupling field as right-hand-polarized (σ^+), while the weak probe field is left-hand-polarized (σ^-).

Using the rotating-wave and the electric dipole approximations, the Hamiltonian of the system in the interaction picture can be written as follows (with units of $\hbar = 1$) [32, 43]:

$$H_{\text{int}} = -\Delta_p |2\rangle \langle 2| + (\Delta_p - \Delta_c) |3\rangle \langle 3| - (\Omega_1 |2\rangle \langle 1| + \Omega_1 |2\rangle \langle 3| + H.c), \tag{1}$$

Using the Liouville equation and the Weisskopf–Wigner theory of spontaneous emission, we obtain the density matrix equations as follows [21, 32]:

$$\dot{\rho}_{11} = i\Omega_1(\rho_{21} - \rho_{12}) + 2\gamma_{21}\rho_{22} + 2\gamma_{31}(\rho_{33} - \rho_{11}) - 2R\rho_{11}, \tag{2a}$$

$$\dot{\rho}_{22} = i\Omega_1(\rho_{12} - \rho_{21}) + i\Omega_2(\rho_{32} - \rho_{23}) - 2(\gamma_{21} + \gamma_{23})\rho_{22} + 2R\rho_{11}, \tag{2b}$$

$$\dot{\rho}_{33} = i\Omega_2(\rho_{23} - \rho_{32}) + 2\gamma_{23}\rho_{22} + 2\gamma_{31}(\rho_{11} - \rho_{33}), \tag{2c}$$

$$\dot{\rho}_{21} = -(R - i\Delta_c + \gamma_{21} + \gamma_{23})\rho_{21} + i\Omega_1(\rho_{11} - \rho_{22}) + i\Omega_2\rho_{31}, \tag{2d}$$

$$\begin{aligned} \dot{\rho}_{31} &= -(R + i(\Delta_p - \Delta_c) + \gamma_{31})\rho_{31} - i\Omega_1\rho_{32} \\ &\quad + i\Omega_2\rho_{21} - 2\eta\sqrt{\gamma_{21}\gamma_{23}}\cos\theta\rho_{22}, \tag{2e} \\ \dot{\rho}_{23} &= -(i\Delta_c + \gamma_{21} + \gamma_{23})\rho_{23} + i\Omega_1\rho_{32} - i\Omega_2(\rho_{22} - \rho_{33}), \tag{2f} \end{aligned}$$

where the matrix elements $\rho_{ij} = \rho_{ij}^*$ (with $i \neq j$) and normalized condition $\rho_{11} + \rho_{22} + \rho_{33} = 1$, respectively; $\Delta_p = \omega_{21} - \omega_p$, and $\Delta_c = \omega_{23} - \omega_c$ indicate atom–field detunings of the probe and the coupling field, respectively. Here, γ_{21} and γ_{23} are the spontaneous decay rates from level $|2\rangle$ to levels $|1\rangle$ and $|3\rangle$, respectively; γ_{31} is the relaxation decay rate between two lower states, which is small and often ignored in the lambda configuration. However, in the general case, γ_{31} has been included in our model [43]. The term $2\eta\sqrt{\gamma_{21}\gamma_{23}}\cos\theta$ represents the result of cross-coupling between the spontaneous emissions channels $|2\rangle \leftrightarrow |1\rangle$ and $|2\rangle \leftrightarrow |3\rangle$, i.e., the SGC effect. The interference parameter p denotes the alignment of the two dipole moments, defined as $p = \vec{\mu}_{21} \cdot \vec{\mu}_{23} / |\vec{\mu}_{21}| |\vec{\mu}_{23}| = \cos\theta$ (with θ being the angle between the two dipole moments), and it represents the strength of the interference between spontaneous emissions. Therefore, the interference is greatest for the parallel dipole moments, while for the perpendicular dipole moments, there is no such interference. If $\eta = 1$, the SGC has to be taken into account, and the strength of SGC will vary versus θ ; otherwise, $\eta = 0$, and the effect of SGC vanishes. Because of the existence of the SGC effect, i.e., of $2\eta\sqrt{\gamma_{21}\gamma_{23}}\cos\theta\rho_{22}$, the properties of the atomic system depend not only on the amplitudes and detunings of the applied fields but also on their phases. Consequently, Rabi frequencies must be regarded as complex parameters. Hence, if the notations φ_p and φ_c are the phases of the probe field and the coupling field, respectively, and $\phi = \varphi_p - \varphi_c$ is the phase difference between the probe field and coupling field, then Ω_1 and Ω_2 can be written as $\Omega_1 = \Omega_p \exp(-i\varphi_p)$ and $\Omega_2 = \Omega_c \exp(-i\varphi_c)$, respectively, where Ω_p and Ω_c are real. Redefining atomic variables in Eq. (2) as $\rho_{ii} = \rho_{ii}$, $\tilde{\rho}_{21} = \rho_{21}e^{i\varphi_p}$, $\tilde{\rho}_{23} = \rho_{23}e^{i\varphi_c}$, and $\tilde{\rho}_{31} = \rho_{31}e^{i\phi}$, we obtain the equations of motion for the redefined density matrix elements $\tilde{\rho}_{ii}$, which are found to be identical to Eq. (2) except that η , Ω_1 and Ω_2 are replaced by $\eta_\phi = \eta e^{i\phi}$, Ω_p and Ω_c , respectively. With the notations ρ_{ij} being reused instead of writing $\tilde{\rho}_{ij}$, the system of equations (2) becomes:

$$\dot{\rho}_{11} = i\Omega_p(\rho_{21} - \rho_{12}) + 2\gamma_{21}\rho_{22} + 2\gamma_{31}(\rho_{33} - \rho_{11}) - 2R\rho_{11}, \tag{3a}$$

$$\dot{\rho}_{22} = i\Omega_p(\rho_{12} - \rho_{21}) + i\Omega_c(\rho_{32} - \rho_{23}) - 2(\gamma_{21} + \gamma_{23})\rho_{22} + 2R\rho_{11}, \tag{3b}$$

$$\dot{\rho}_{33} = i\Omega_c(\rho_{23} - \rho_{32}) + 2\gamma_{23}\rho_{22} + 2\gamma_{31}(\rho_{11} - \rho_{33}), \tag{3c}$$

$$\dot{\rho}_{21} = -(R - i\Delta_c + \gamma_{21} + \gamma_{23})\rho_{21} + i\Omega_p(\rho_{11} - \rho_{22}) + i\Omega_c\rho_{31}, \tag{3d}$$

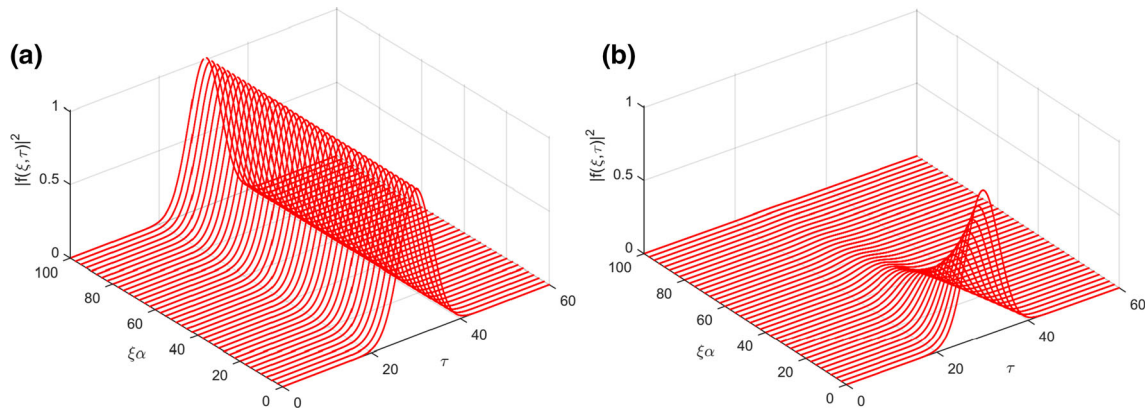


Fig. 2 Spatiotemporal evolution of the probe pulse intensity when the coupling field is turned on (a) and turned off (b). Other parameters are $\Omega_{p0} = 0.1\gamma_{21}$, $\Omega_c = 5\gamma_{21}$, $\Delta_p = \Delta_c = 0$, $p = 0$, $R = 0$, $\phi = 0$, and $\gamma_{23} = \gamma_{21}$, respectively

$$\dot{\rho}_{31} = -(R + i(\Delta_p - \Delta_c) + \gamma_{31})\rho_{31} - i\Omega_p\rho_{32} + i\Omega_c\rho_{21} - 2p\sqrt{\gamma_{21}\gamma_{23}}\eta_\phi\rho_{22}, \quad (3e)$$

$$\dot{\rho}_{23} = -(i\Delta_c + \gamma_{21} + \gamma_{23})\rho_{23} + i\Omega_p\rho_{32} - i\Omega_c(\rho_{22} - \rho_{33}), \quad (3f)$$

Under the slowly varying envelope and the rotating-wave approximation, the propagation of the probe field in the atomic medium is governed by Maxwell’s wave equations as follows:

$$\frac{\partial\Omega_p(z, t)}{\partial z} + \frac{1}{c}\frac{\partial\Omega_p(z, t)}{\partial t} = i\alpha\gamma_{21}\rho_{21}(z, t), \quad (4)$$

where $\alpha = \frac{\omega_p N |d_{21}|^2}{4\epsilon_0 c \hbar \gamma_{21}}$ is the propagation constant. It is convenient to transform Eqs. (3) and (4) in the local frame by changing $\xi = z$ and $\tau = t - z/c$, with c being the speed of light in vacuum. In this frame, Eqs. (3) stay unchanged with the substitution of $t \rightarrow \tau$ and $z \rightarrow \xi$, while Eq. (4) is rewritten as [27]:

$$\frac{\partial\Omega_p(\xi, \tau)}{\partial \xi} = i\alpha\gamma_{21}\rho_{21}(\xi, \tau), \quad (5)$$

The proposed model can be applied to the ^{87}Rb atom, with the corresponding shifts 5S–5P. The designated states and the decay rates can be selected as follows [45]: $|1\rangle = |5S_{1/2}, F = 1\rangle$, $|2\rangle = |5P_{1/2}, F = 1\rangle$, $|3\rangle = |5S_{1/2}, F = 2\rangle$, and $\gamma = \gamma_{21} = \gamma_{23} = 6 \text{ MHz}$, $\gamma_{31} = 0.05\gamma_{21}$, and the wavelength of the probe field and coupling field, $\lambda_p = \lambda_c = 780 \text{ nm}$, respectively.

3 Results and discussion

In this section, we use the Bloch–Maxwell Eqs. (3a)–(3f) and (5) to simulate the pulse propagation dynamics and the optical switching of the probe field according to the coupling laser field. The initial condition assumes that

all atoms are in the ground state $|1\rangle$, namely $\rho_{11}(\xi, \tau = 0) = 1$, and the boundary condition assumes that the probe field is a Gaussian-type pulse $f(\xi = 0, \tau) = \exp[-(\ln 2)(\tau - 30)^2/\tau_0^2]$, with $\tau_0 = 6/\gamma_{21}$ being the temporal width of the Gaussian pulse at the beginning in the medium.

First, we investigate pulse propagation in the case where both the SGC and incoherent pump field are absent, and find the soliton shape of the probe pulse under EIT conditions. Figure 2 illustrates the spatiotemporal evolution of the squared magnitude of the normalized probe pulse envelope $|f(\xi, \tau)|^2$ without an incoherent pump when the coupling field is ON (a) and OFF (b). The selected parameters are $\Omega_{p0} = 0.1\gamma_{21}$, $\Omega_c = 5\gamma_{21}$, $\Delta_p = \Delta_c = 0$, $\phi = 0$ and $p = 0$ (no SGC). From Fig. 2a, it can be seen that when the coupling field is ON, the medium is transparent to the probe field, so the probe pulse propagates via the medium almost without attenuation, which means that the EIT effect occurs, and the probe pulse can still maintain its shape over a relatively long propagation distance. Conversely, when the coupling field is OFF (and hence no EIT for the probe field), the medium becomes opaque for the probe field, and thus the probe pulse is attenuated extremely rapidly upon entering the medium, as shown in Fig. 2b. This is the key mechanism for AOS through the modulation of the coupling field.

Now, we study the influence of SGC, relative phase and incoherent field on the optical switching behavior of the probe field modulated by the coupling field, as illustrated in Figs. 3, 4, 5 and 6 below. In order to investigate the influence of SGC on the optical switching behavior of the probe field, the temporal evolution of the probe field is constructed at the propagation distance $\xi = 50/\alpha$ for different values of the parameters p as shown in Fig. 3. Here, the relative phase is zero ($\phi = 0$) and an incoherent field is absent ($R = 0$), the temporal evolution of the probe field (blue solid line) is assumed to be a continuous wave, and the switching coupling field (red dashed line) is modulated by a nearly square pulse with smooth rising and falling edges, and

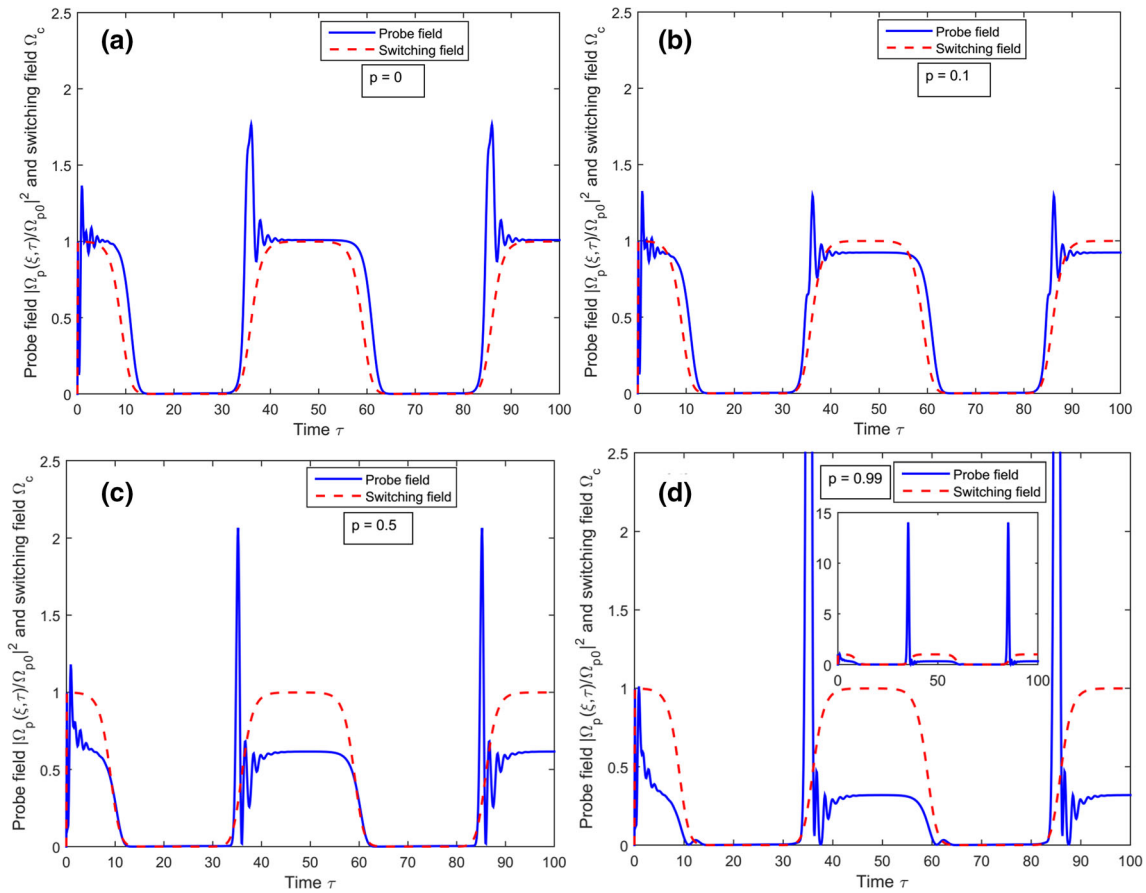


Fig. 3 Temporal evolution of the continuous-wave probe field (blue solid line) and the switching coupling field (red dashed lines) at the propagation distance $\xi = 50/\alpha$ for different values of the parameter p : **a** $p = 0$, **b** $p = 0.1$, **c** $p = 0.5$, **d** $p = 0.99$. Other parameters are the same as those in Fig. 2a

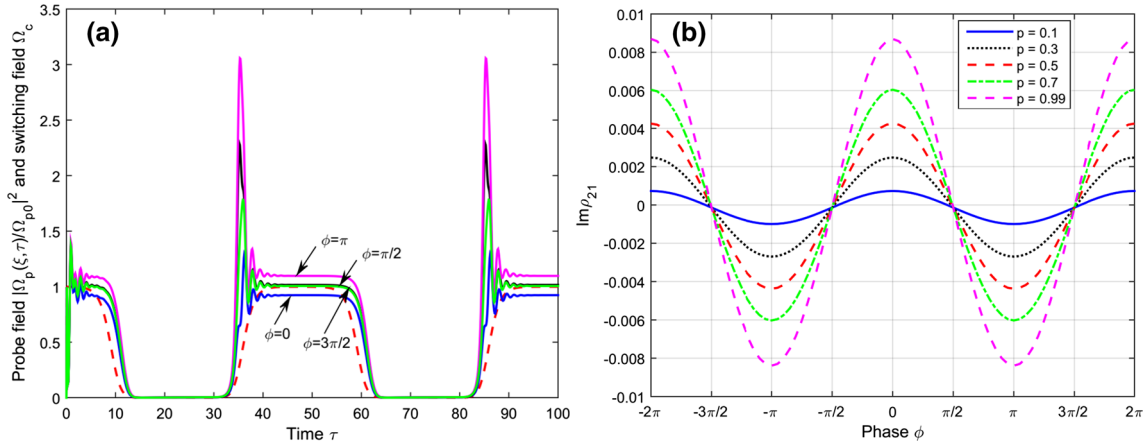


Fig. 4 a Time evolution of the continuous-wave probe field (solid line) and the switching coupling field (dashed lines) at the propagation distance $\xi = 50/\alpha$ for different values of the relative phase ϕ when $p = 0.1$, and **b** the absorption coefficient $\text{Im}(\rho_{21})$ versus the relative phase ϕ for different values of the parameter p . Other parameters are the same as those in Fig. 2a

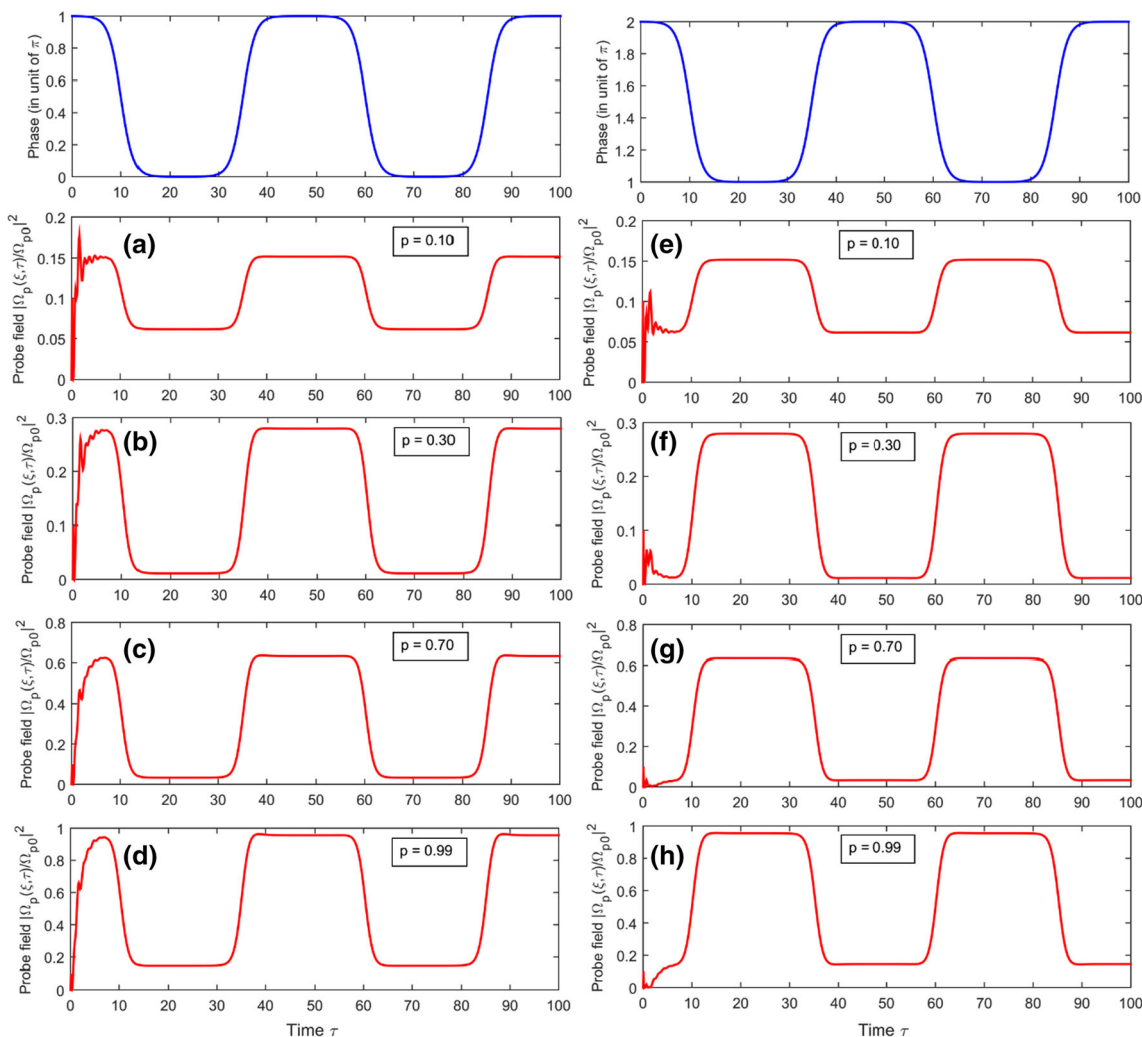


Fig. 5 Time evolution of the continuous-wave probe field (red line) at $\xi = 100/\alpha$ versus the modulation of the relative phase $\phi(\tau)$ (blue lines) in two ranges of the relative phase ϕ for the different values of the SGC parameter p : from 0 to π for (a–d), and from π to 2π for (e–h). The other parameters are given by $\Omega_p = 0.1\gamma_{21}$, $\Omega_c = 5\gamma_{21}$, $R = 0.05$, $\Delta_p = \Delta_c = 0$, and $\gamma_{23} = \gamma_{21}$, respectively

is the function of τ [44]:

$$\Omega_c(\tau) = \Omega_{c0} \left\{ \begin{array}{l} 1 - 0.5 \tanh [0.4(\tau - 10)] \\ +0.5 \tanh [0.4(\tau - 35)] \\ -0.5 \tanh [0.4(\tau - 60)] \\ +0.5 \tanh [0.4(\tau - 85)] \end{array} \right\}, \quad (6)$$

which is normalized by its peak value $\Omega_{c0} = 5\gamma_{21}$. The switching coupling field is turned on or off at an approximate period of $50/\gamma_{21}$. Figure 3 shows that the probe field transmission can exhibit the ON or OFF mode when the coupling field is turned ON or OFF, respectively. It also shows that the SGC has a strong influence on the switching process of the probe field. Specifically, when the SGC is small, $p = 0.1$ (Fig. 3b), the switching efficiency is reduced compared to the case without SGC, $p = 0$ (Fig. 3a), while the oscillations at the front edge of the probe pulse are significantly

reduced. However, when increasing the strength of the SGC (by increasing the parameter p), the oscillations at the front edge of the probe pulse become extremely large and the switching efficiency drops dramatically. This means that the switching probe field is significantly attenuated by the atomic medium, as shown in Fig. 3c, d. These physical phenomena can be explained based on the influence of SGC on EIT and dispersion as follows [32]: As the parameter p increases, the depth of the EIT window (for the probe field) also increases, but its width is narrower. That is, the absorption on both sides of the EIT window also increases. This results in the dispersion becoming steeper but its height decreasing as p increases. Therefore, there is always competition between the height and slope of the dispersion when increasing the parameter p . The dispersion can create oscillations in the front edge of the switching probe pulse [29, 44], while the strong absorption on

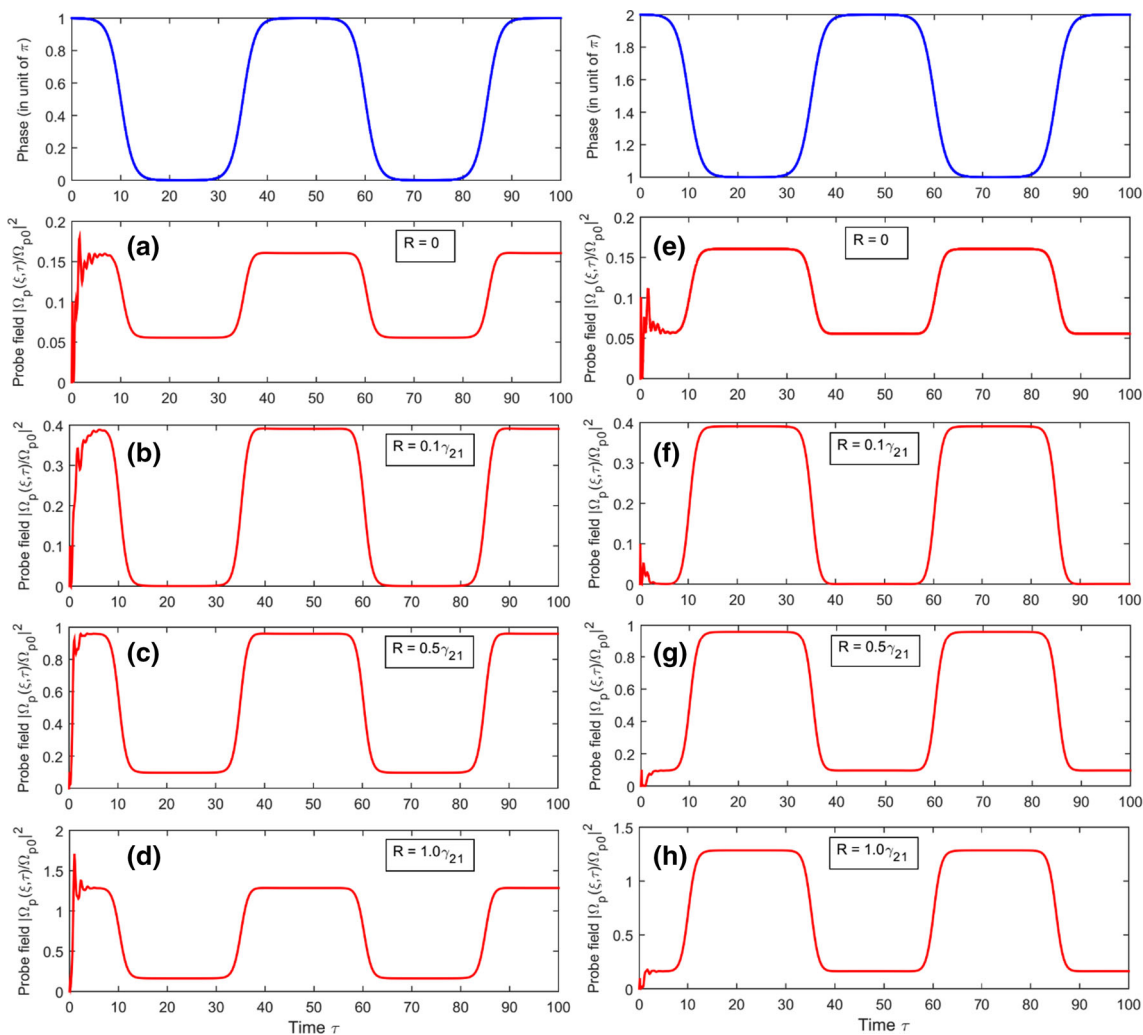


Fig. 6 Time evolution of the continuous-wave probe field (red line) at $\xi = 100/\alpha$ versus the modulation of the relative phase $\phi(\tau)$ (blue lines) in the two ranges of the relative phase ϕ for the different values of the incoherent pumping rate R : from 0 to π for (a–d), and from π to 2π for (e–h). The other parameters are given by $\Omega_p = 0.1\gamma_{21}$, $\Omega_c = 5\gamma_{21}$, $p = 0.3$, $\Delta_p = \Delta_c = 0$, and $\gamma_{23} = \gamma_{21}$, respectively

both sides of the EIT window (together with the narrowing of the EIT spectral domain) leads to a decrease in the efficiency of the switching probe field, as seen in Fig. 3.

Figure 4a shows the influence of the relative phase ϕ on the switching probe behaviors in the presence of SGC (with $p = 0.1$) and the absence of incoherent pumping field. Here, the switching coupling field (red dashed line) is modulated by a nearly square pulse with smooth rising and falling edges, and has the same form as Eq. (6). In Fig. 4b we plot the absorption coefficient, $\text{Im}(\rho_{21})$, versus the relative phase ϕ for different values of the parameter p . From Fig. 4a, it can be observed the switching probe pulse is also quite sensitive to change in the relative phase ϕ : when $\phi = 0$, the probe field is switched to a nearly square pulse with reduced amplitude due to strong probe absorption at $\phi = 0$ (see Fig. 4b); on the contrary, when $\phi = \pi$, the amplitude of the switching probe field is enhanced due

to the probe amplification at $\phi = \pi$ (see Fig. 4b); with $\phi = \pi/2$, the switching probe field presents very small absorption, which is similar to the case without SGC; at $\phi = 3\pi/2$, the switching probe field is the same as that of $\phi = \pi/2$. Thus, in the presence of the SGC, highly efficient switching can be obtained if an appropriate phase value is selected.

On the other hand, from Fig. 4b, the graph of the probe absorption is observed to be identical to a sine graph with a period of 2π . When relative phase $\phi = k\pi$ ($k = 0, 1, 2, \dots$), the medium exhibits maximum absorption or amplification for the probe field. When relative phase $\phi = (2k + 1)\pi/2$, the medium becomes transparent to the probe field. Thus, by changing the relative phase, the medium can be switched from the maximum absorption regime to the transparency regime. This is a great idea to create optical switching for the probe field versus the relative phase. Indeed, Fig. 5 demonstrates the continuous-wave probe field

which is modulated with relative phase $\phi(\tau)$ by a near-square pulse with smooth rising and falling edges [43]:

$$\phi(\tau) = \pi\{a_n - 0.5[\tanh 0.4(\tau - 10) - \tanh 0.4(\tau - 35) + \tanh 0.4(\tau - 60) - \tanh 0.4(\tau - 85)]\}, \quad (7)$$

where $a_n = 1, \text{ and } 2$, corresponding to the modulation of the relative phase in the ranges $0-\pi$ and $\pi-2\pi$, respectively. Figure 5 describes the dependence of the on-off state of the probe field on the modulation of the relative phase for different values of parameter p in the presence of an incoherent pumping. It is shown that the on-off state of probe field transmission relies on the switching mode of the relative phase. Specifically, in the range $0-\pi$ of the relative phase, the probe field is switched to the ON or OFF mode when the relative phase is switched to the ON or OFF mode, respectively (see Fig. 5a-d), and the probe field is switched synchronously with the relative phase. However, in the range $\pi-2\pi$ of the relative phase, the probe field is switched anti-synchronously with the relative phase (see Fig. 5e-h). At the same time, the switching efficiency increases gradually and achieves the maximum value when the parameter p reaches the maximum value of $p = 0.99$ (see Fig. 5d and h). In these cases, the switching efficiency is increased with the increase in parameter p . The physical reason for the synchronous or anti-synchronous switching phenomenon can be explained as follows: From Fig. 4b, in the range $0-\pi$, the absorption coefficient varies from a positive extreme to zero and then to a negative extreme, so the probe field is also switched from OFF mode (corresponding to the positive extreme of absorption) to ON mode (corresponding to zero absorption) and then to OFF mode (at the negative extreme of absorption). This means that the probe field is switched synchronously with the relative phase. The same explanation applies for the anti-synchronous switching phenomenon in the range $\pi-2\pi$.

Finally, we present the influence of incoherent pumping on the probe field switching versus the relative phase when the parameter $p = 0.3$, as shown in Fig. 6, where other parameters used are given the same as in Fig. 5. This shows that in the range $0-\pi$, the switching of the probe field is synchronous (see Fig. 6a-d), while in the range $\pi-2\pi$, the switching is anti-synchronous (see Fig. 6e-h) with the relative phase. In both cases, the switching efficiency is greatly increased when increasing the incoherent pumping rate. Indeed, when $R = 0$, the switching probe pulse is significantly attenuated (see Fig. 6a and e). However, in the presence of incoherent pumping ($R \neq 0$), the switching efficiency increases when the incoherent pumping rate is increased (see Fig. 6b-d and f-h). At the same time, the amplitude of the switching probe pulse can be converted from absorption to amplification regimes. Thus, the incoherent pumping field plays an important role in

enhancing the switching efficiency of the probe switching. This can be explained as follows: in Fig. 1, the probe field is much weaker than the coupling field, so the population is mainly in the state $|1\rangle$. The presence of the incoherent pumping field will shift the population from the level $|1\rangle$ to the level $|2\rangle$ (increased incoherent pumping rate, the population in the level $|2\rangle$ also increases). This will increase the efficiency of quantum interference that is created by cross-coupling between spontaneously emission channels or SGC. Therefore, the switching efficiency of the probe field (versus relative phase) increases with the increase in the incoherent pumping rate. Thus, although SGC can damage the switching signal, by choosing the appropriate phase and incoherent pumping rate, we can optimize the signal and perfect the optical switching performance.

4 Conclusion

In summary, the target of this study was the switching of the probe field by phase switching based on the effect of spontaneously generated coherence. A near-square pulse from a continuous wave of the probe field was formed with a similar modulation period of coupling field intensity or the relative phase. The switching efficiency by the relative phase was enhanced with the increase in the strength of spontaneously generated coherence in the presence of incoherent pumping. In addition, the incoherent pumping significantly reduced absorption and increased switching efficiency in the phase domains. The results show that choosing the appropriate values for the spontaneously generated coherence, range of the relative phase, incoherent pumping rate and intensity of the applied fields can achieve optimal probe field switching performance.

Acknowledgements Financial support from the Ministry of Education and Training under Grant No. B2018-TDV-01SP.

Author contributions

NTTH and HMD created the research model, developed the theory and performed calculations. All authors co-wrote the paper, discussed the results and contributed equally to the final manuscript.

Data Availability Statement This manuscript has no associated data or the data will not be deposited. [Authors' comment: No datasets were generated or analyzed during the current study. The results are based on the theoretical study.]

Declarations

Conflict of interest The authors declare no conflict of interest.

References

1. H. Ishikawa, *Ultrafast all-optical signal processing devices* (Wiley, Singapore, 2008)
2. A. Imamoglu, S.E. Harris, Lasers without inversion: interference of dressed lifetime broadened states. *Opt. Lett.* **14**, 1344–1346 (1989)
3. K.J. Boller, A. Imamoglu, S.E. Harris, Observation of electromagnetically induced transparency. *Phys. Rev. Lett.* **66**, 2593 (1991)
4. B.-W. Shiau, M.-C. Wu, C.-C. Lin, Y.-C. Chen, Low-light-level cross-phase modulation with double slow light pulses. *Phys. Rev. Lett.* **106**, 193006 (2011)
5. V. Venkataraman, K. Saha, A.L. Gaeta, Phase modulation at the few-photon level for weak-nonlinearity-based quantum computing. *Nat. Photon.* **7**, 138–141 (2013)
6. L.V. Hau, S.E. Harris, Z. Dutton, C.H. Bejroozi, Light speed reduction to 17 meters per second in an ultracold atomic gas. *Nature* **397**, 594–598 (1999)
7. D.F. Phillips, A. Fleischhauer, A. Mair, R.L. Walsworth, M.D. Lukin, Storage of light in atomic vapor. *Phys. Rev. Lett.* **86**, 783 (2001)
8. A. Joshi, A. Brown, H. Wang, M. Xiao, Controlling optical bistability in a three-level atomic system. *Phys. Rev. A* **67**, 041801(R) (2003)
9. S.E. Harris, Lasers without inversion: interference of lifetime broadened resonances. *Phys. Rev. Lett.* **62**, 1033–1036 (1989)
10. Y. Mu, L. Qin, Z. Shi, G. Huang, Giant Kerr nonlinearities and magneto-optical rotations in a Rydberg-atom gas via double electromagnetically induced transparency. *Phys. Rev. A* **103**, 043709 (2021)
11. H.M. Dong, N.T. Anh, T.D. Thanh, Controllable Kerr nonlinearity in a degenerate V-type inhomogeneously broadening atomic medium aided by a magnetic field. *Opt Quant Electron.* **54**(4), 225 (2022)
12. R.B. Li, L. Deng, E.W. Hagley, Fast, all-optical, zero to π continuously controllable Kerr phase Gate. *Phys. Rev. Lett.* **110**, 113902 (2013)
13. H.M. Dong, L.T.Y. Nga, D.X. Khoa, N.H. Bang, Controllable ultraslow optical solitons in a degenerated two-level atomic medium under EIT assisted by a magnetic field. *Sci. Rep.* **10**, 15298 (2020)
14. J.H. Li, R. Yu, X. Yang, Phase-controlled absorption-gain properties and optical switching in nanodiamond nitrogen-vacancy center. *Appl. Phys. B* **111**, 65–73 (2013)
15. L.-G. Si, Lu. Xin-You, X. Hao, J.-H. Li, Dynamical control of soliton formation and propagation in a Y-type atomic system with dual ladder-type electromagnetically induced transparency. *J. Phys. B At. Mol. Opt. Phys.* **43**, 065403 (2010)
16. Yu. Rong, J. Li, C. Ding, X. Yang, Dual-channel all-optical switching with tunable frequency in a five-level double-ladder atomic system. *Opt. Commun.* **284**, 2930 (2011)
17. Y. Chen, Z. Bai, G. Huang, Ultraslow optical solitons and their storage and retrieval in an ultracold ladder-type atomic system. *Phys. Rev. A* **89**, 023835 (2014)
18. H.M. Dong, L.V. Doai, V.N. Sau, D.X. Khoa, N.H. Bang, Propagation of laser pulse in a three-level cascade atomic medium under conditions of electromagnetically induced transparency. *Photon. Lett. Pol.* **3**, 73 (2016)
19. D.X. Khoa, H.M. Dong, L.V. Doai, N.H. Bang, Propagation of laser pulse in a three-level cascade inhomogeneously broadened medium under electromagnetically induced transparency conditions. *Optik* **131**, 497 (2017)
20. H.R. Hamed, Optical switching, bistability and pulse propagation in five-level quantum schemes. *Laser Phys.* **27**, 066002 (2017)
21. H.M. Dong, L.V. Doai, N.H. Bang, Pulse propagation in an atomic medium under spontaneously generated coherence, incoherent pumping, and relative laser phase. *Opt. Commun.* **426**, 553–557 (2018)
22. H. Schmidt, R.J. Ram, All-optical wavelength converter and switch based on electromagnetically induced transparency. *Appl. Phys. Lett.* **76**, 3173 (2000)
23. A. Fountoulakis, A.F. Terzis, E. Paspalakis, All-optical modulation based on electromagnetically induced transparency. *Phys. Lett. A* **374**, 3354 (2010)
24. R. Yu, J. Li, P. Huang, A. Zheng, X. Yang, Dynamic control of light propagation and optical switching through an RF-driven cascade-type atomic medium. *Phys. Lett. A* **373**, 2992 (2009)
25. J.H. Li, R. Yu, Y. Wu, Propagation of magnetically controllable lasers and magneto-optic dual switching using nitrogen-vacancy centers in diamond. *J. Appl. Phys.* **113**, 103104 (2013)
26. H. Jafarzadeh, All-optical switching in an open V-type atomic system. *Laser Phys.* **27**, 025204 (2017)
27. H.M. Dong, L.T.Y. Nga, N.H. Bang, Optical switching and bistability in a degenerated two-level atomic medium under an external magnetic field. *Appl. Opt.* **58**, 4192 (2019)
28. N.T. Anh, T.D. Thanh, N.H. Bang, H.M. Dong, Microwave-assisted all-optical switching in a four-level atomic system. *Pramana J. Phys.* **95**, 37 (2021)
29. D.X. Khoa, N.V. Ai, H.M. Dong, L.V. Doai, N.H. Bang, All-optical switching in a medium of a four-level vee-cascade atomic medium. *Opt Quant Electron.* **54**(3), 164 (2022)
30. J. Javanainen, Effect of state superpositions created by spontaneous emission on laser-driven transitions. *Europhys. Lett.* **17**, 407 (1992)
31. H.M. Ma, S.Q. Gong, C.P. Liu, Z.R. Sun, Z.Z. Xu, Effects of spontaneous emission-induced coherence on population inversion in a ladder-type atomic system. *Opt. Commun.* **223**, 97 (2003)
32. J.H. Wu, J.Y. Gao, Phase control of light amplification without inversion in a Λ system with spontaneously generated coherence. *Phys. Rev. A* **65**, 063807 (2002)
33. C.P. Liu, S.Q. Gong, X.J. Fan, Z.Z. Xu, Electromagnetically induced absorption via spontaneously generated coherence of a Λ system. *Opt. Commun.* **231**, 289–295 (2004)
34. M. Sahrai, The effect of the spontaneously generated coherence on the dynamical behaviors of the dispersion and the absorption. *Eur. Phys. J. Spec. Topics* **160**, 383 (2008)

35. C. Ni, F.X. Jun, L.A. Yun, L.C. Pu, G.S. Qing, X.Z. Zhan, Phase control in an open Λ -type system with spontaneously generated coherence. *Chin. Phys* **16**(3), 1009–1963 (2007)
36. X.J. Fan, A.Y. Li, F.G. Bu, H.X. Qiao, J. Du, Z.-Z. Xu, Phase-dependent properties for absorption and dispersion in a closed equispaced three-level ladder system. *Optik* **119**, 540 (2008)
37. Y. Bai, H. Guo, D. Han, H. Sun, Effects of spontaneously generated coherence on the group velocity in a V system. *Phys. Lett. A* **340**, 342 (2005)
38. M. Mahmoudi, M. Sahrai, H. Tajalli, The effects of the incoherent pumping field on the phase control of group velocity. *J. Phys. B At. Mol. Opt. Phys.* **39**, 1825 (2006)
39. Y.P. Niu, S.Q. Gong, Enhancing Kerr nonlinearity via spontaneously generated coherence. *Phys. Rev. A* **73**, 053811 (2006)
40. Y. Bai, T. Liu, X. Yu, Giant Kerr nonlinearity in an open V-type system with spontaneously generated coherence. *Optik* **124**, 613 (2012)
41. D.-c Cheng, C.-p Liu, S.-q Gong, Optical bistability and multistability via the effect of spontaneously generated coherence in a three-level ladder-type atomic system. *Phys. Lett. A* **332**, 244 (2004)
42. H. Kang, G. Hernandez, J. Zhang, Y. Zhu, Phase-controlled light switching at low light levels. *Phys. Rev. A* **73**, 011802(R) (2006)
43. H.M. Dong, N.H. Bang, Controllable optical switching in a closed-loop three-level lambda system. *Phys. Scr.* **94**, 115510 (2019)
44. H.M. Dong, N.H. Bang, D.X. Khoa, L.V. Doai, All-optical switching via spontaneously generated coherence, relative phase and incoherent pumping in a V-type three-level system. *Opt. Commun.* **507**, 127731 (2022)
45. D.A. Steck, 87Rb D line data (2019). <http://steck.us/alkalidata>

Springer Nature or its licensor (e.g. a society or other partner) holds exclusive rights to this article under a publishing agreement with the author(s) or other rightsholder(s); author self-archiving of the accepted manuscript version of this article is solely governed by the terms of such publishing agreement and applicable law.